IEEE Access
Multidisciplinary | Rapid Review | Open Access Journal

Received December 20, 2019, accepted December 27, 2019, date of publication January 9, 2020, date of current version January 17, 2020.

Digital Object Identifier 10.1109/ACCESS.2020.2965177

Analysis of a Quadcopter's Acoustic Signature in Different Flight Regimes

IVAN DJUREK, (Member, IEEE), ANTONIO PETOSIC, SANJA GRUBESA, AND MIA SUHANEK

Department of Electroacoustics, Faculty of Electrical Engineering and Computing, University of Zagreb, 10000 Zagreb, Croatia

Corresponding author: Ivan Djurek (ivan.djurek@fer.hr)

This work was supported in part by the European Union from the European Regional Development Fund (ERDF) under Project KK.01.2.1.01.0103 4D Acoustical Camera (in Croatian: 4D Akustička kamera).

ABSTRACT This paper presents a detailed analysis of quadcopter noise emitted in different flight regimes and suggests an innovative approach to quadcopter sound detection. Currently, quadcopters have become extremely popular and are used for various applications. In some case scenarios, these applications are not legal; therefore, they represent a threat, and early detection of quadcopters becomes imperative. However, conventional detection with radars and infrared cameras does not provide satisfactory results, since some quadcopters have relatively small dimensions, and their motors have low heat emissions. Thus, this paper focuses on the noise emitted by quadcopters, which is connected to the changing revolutions per minute of the electric quadcopter motors. Thus, the paper connects the unique quadcopter features with the emitted sounds, which can be used for detection in different acoustic environments. The suggested algorithm uses signal processing with a nonlinear function, which results in new spectral lines that correspond to rotational speed differences between the front and rear motors. The analysis shows that the processed signal mixed with a traffic noise signal can be detected when the level reaches 3 dB lower than the level of the surrounding noise.

INDEX TERMS Quadcopter, drone, detection, noise, characteristic sound print, time and frequency analysis.

I. INTRODUCTION

Nowadays, Currently, the increasing popularity of small unmanned aerial vehicles (UAVs), particularly quadcopters, has resulted in various applications and uses of the aforementioned vehicles. Although these vehicles are mainly used for commercial or hobbyist purposes, reports show an increase in their use for several illegal activities [1]. A relatively small quadcopter (i.e., a special and popular UAV design version that includes four motors) could potentially pose a serious threat in various environments; e.g., they are often used for smuggling purposes. On the other hand, larger quadcopter units could carry small amounts of explosives. Recently, there were several cases in which small quadcopters caused airport shutdowns and flight delays [2].

Due to their size, it is very challenging to detect quadcopters. Their small frontal surface and large use of plastic for construction make quadcopters difficult to detect with conventional radars. The selection of the radar wavelength is very important, and certain conditions must be fulfilled, which in some cases do not correspond to real-life situations [3], [4]. In certain areas, such as airports, the operation of additional radars could be dangerous. If radars are used for detection, a bird could be identified as a UAV, which could activate a false alarm.

On the other hand, small electric motors emit very small amounts of heat, and therefore, detection with infrared (IR) cameras is also difficult to achieve. Detection systems that monitor radio frequencies are limited to quadcopters that are remotely controlled. Global positioning system (GPS)-controlled quadcopters are a real and true threat, as they cannot be detected with any of these systems.

A method that recently acquired great interest is the detection of unmanned aerial vehicles by analyzing the sounds that they emit. The analysis of emitted sound in combination with a radar signal could ensure the precise and reliable detection of quadcopters. Quadcopters and small rotor-driven UAVs have a characteristic broadband sound. The sound of rotor

The associate editor coordinating the review of this manuscript and approving it for publication was Jiankang Zhang.

blades is an impulse sound rich in harmonics [5], and because various detection methods rely on this fact, there are several papers describing different studies for the detection of UAVs. For example, in [6], the authors propose the detection of quadcopters (drones) based on a hidden Markov model using the Mel Frequency Cepstral Coefficient (MFCC) technique. This method showed relatively good results in noisy environments; however, the method requires a database of specific sounds, which then limits the method's application. Similarly, the methods described in [7], which use signal correlation to detect quadcopter sounds, also require previously recorded sample signals. In real-life situations, when it is necessary to detect a quadcopter at a relatively large distance, the sound signal would have a low signal-to-noise ratio, and its comparison with sample signals will always result in a low correlation factor.

The analysis of the acoustic signature is an important part of any sound detection. This analysis usually involves the extraction of acoustical features based on the frequency spectrum [8]. As mentioned, the frequency spectrum of quadcopters is broad and rich with harmonics, and thus, existing detection methods rely on the detection of harmonics in the sound signal. In noisy environments, this approach can present a challenge. The signal-to-noise ratio must be high so that these signals are detected [9]. This high signal-to-noise ratio represents ideal conditions; however, in "real" acoustic environments, this is usually not the case. To develop a reliable system for protection against quadcopters with malicious purposes, they must be detected in time. If sound detection is used, when quadcopters are far away from a microphone-based detection system, the signal-to-noise ratio is very low. The level of surrounding noise, for example, around airports, could be much higher than the level of quadcopter sound, even if a high-directivity microphone array is used. Therefore, the extraction of the quadcopter acoustic signature from environmental noise requires a more detailed analysis of its sound print.

This paper focuses on a detailed analysis of quadcopter sounds, based on their operation principle, which involves four rotor blades, i.e., four electrical motors. The paper analyses the quadcopter sounds in various flight regimes, which involve hovering and linear forward-backward flight. It was found that the frequency spectrum of the quadcopter sound changes depending on whether it is flying or hovering, which could help in identifying a reliable algorithm for the early detection of quadcopters in the case of a high level of surrounding noise (Figure 1).

II. OPERATIONAL PRINCIPLE OF A QUADCOPTER

Quadcopters use two common types of configurations for controlling their motors, namely, cross-configuration and plus-configuration [10], [11]. These two configurations are different in the definition of the orientation of the quadcopter and motor activation for roll and pitch rotation. In the case of the plus-configuration, two opposite motors control the roll rotation, while the other two control the pitch rotation.

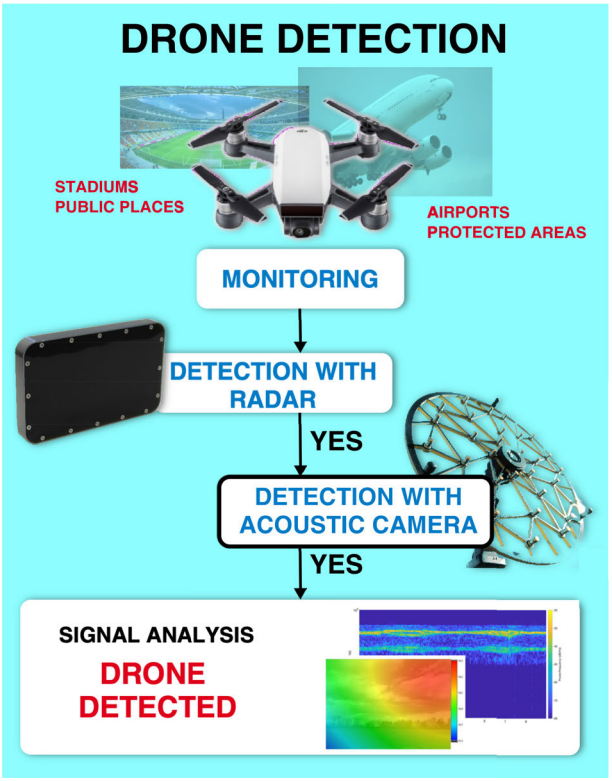

FIGURE 1. Block diagram of the study.

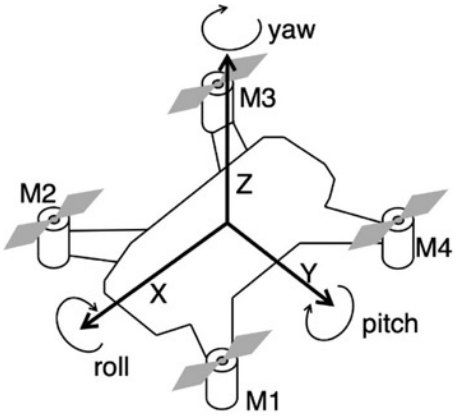

FIGURE 2. Diagram of a quadcopter with two blades per motor.

On the other hand, in the case of the cross-configuration, all four motors control the roll and pitch rotation. In this paper, the cross-configuration is analyzed (i.e., the quadcopter used for experiments implements that configuration); however, the final obtained conclusions from this research can be applied to both configurations. Figure 2 shows a simple diagram of a quadcopter in the cross-configuration, with defined coordinate frames. By changing the rotation speed of the motors, the quadcopter changes its flight regimes.

When placing the origin of the quadcopter's body frame in its center of mass, as shown in Figure 1, the position of the quadcopter r is defined in an inertial frame as

$$r = \begin{bmatrix} r_x & r_y & r_z \end{bmatrix}^T. \tag{1}$$

The orientation (η) of the quadcopter is defined in the body frame as three kinds of rotation around three coordinate axes, namely, roll φ, pitch θ and yaw ψ

$$\eta = \begin{bmatrix} \varphi & \theta & \psi \end{bmatrix}^T. \tag{2}$$

A rotation matrix R performing rotation from the body frame to the inertial frame in ZYX order is defined as

$$R = \begin{bmatrix} c_\theta c_\psi & c_\psi s_\varphi s_\theta - c_\varphi s_\psi & c_\varphi c_\psi s_\theta + s_\varphi s_\psi \\ c_\theta s_\psi & s_\varphi s_\theta s_\psi + c_\varphi c_\psi & c_\psi s_\theta s_\psi - c_\psi s_\varphi \\ -s_\theta & c_\theta s_\varphi & c_\varphi c_\theta \end{bmatrix}, \tag{3}$$

where c and s represent the shorthand cosine and sine functions, respectively.

Analyzing the quadcopter motion, there are several forces acting on it, and in addition to air resistance, the dominant forces are thrust and gravitational force. According to the motors marked in Figure 2, it is possible to define ω_i, the matrix of rotation speeds for the quadcopter motors:

$$\omega_i = \begin{bmatrix} \omega_{\mathrm{M1}} & \omega_{\mathrm{M2}} & \omega_{\mathrm{M3}} & \omega_{\mathrm{M4}} \end{bmatrix}^T. \tag{4}$$

Using Euler's first law of motion for rigid body dynamics, the equation of linear motion of the body can be modeled as

$$\frac{d^2 r}{dt^2} = g \begin{bmatrix} 0 \\ 0 \\ 1 \end{bmatrix} - \frac{RK_T}{M} \sum_{i=1}^{4} \omega_{Mi}^2 \begin{bmatrix} 0 \\ 0 \\ 1 \end{bmatrix}, \tag{5}$$

where g, M and K_T denote the gravitational constant, the mass of the rigid body and the thrust constant of the propeller blades, respectively.

The moving direction of a quadcopter is controlled by the rotation speed of the four motors. When taking into account that there are no roll and yaw changes, the equation of forward linear motion in the direction of the x-axis, derived from equation (5), can be written as

$$\frac{d^2 r_x}{dt^2} = -sin\,(\theta)\,\frac{K_T}{M} \sum_{i=1}^{4} \omega_{Mi}^2. \tag{6}$$

For a quadcopter to move forward, it must overcome the pitch torque T_θ along the y-axis. Since the torque is defined as the lever arm distance L and force, torques that result in changes in the roll and pitch angles are differences in torques along the same body axis:

$$T_\varphi = LK_T \left(\omega_{\mathrm{M1}}^2 - \omega_{\mathrm{M2}}^2 - \omega_{\mathrm{M3}}^2 + \omega_{\mathrm{M4}}^2 \right), \tag{7}$$

$$T_\theta = LK_T \left(\omega_{\mathrm{M1}}^2 + \omega_{\mathrm{M2}}^2 - \omega_{\mathrm{M3}}^2 - \omega_{\mathrm{M4}}^2 \right). \tag{8}$$

To fly, a quadcopter must constantly monitor and correct the rotation speed of its motors. Even a small wind could induce the necessary correction of motor speed. This phenomenon is even more noticeable in linear forward, backward and side flights. In these case scenarios, the difference in the rotation speed determines the velocity of the quadcopter's motion with respect to the ground. In the case of vertical flight, these differences are smaller; however, they are still evident.

For example, if a quadcopter flies forward, the following relationship among rotation speeds, i.e., corresponding frequencies, must be valid when taking into account the markings shown in Figure 2

$$\omega_{\mathrm{M3}} = \omega_{\mathrm{M4}} > \omega_{\mathrm{M1}} = \omega_{\mathrm{M2}}. \tag{9}$$

If a quadcopter flies left, the relationship among rotation speeds is as follows:

$$\omega_{\mathrm{M1}} = \omega_{\mathrm{M4}} > \omega_{\mathrm{M2}} = \omega_{\mathrm{M3}}. \tag{10}$$

The same principle can be used for backward flying and flying to the right. Hence, if the quadcopter is moving, there are rotation speed differences between the front and rear and the left and right motors. This feature distinguishes quadcopters from other propeller-based UAVs.

Using the basic laws of physics [12]–[15] while neglecting wind influence, an equation can be written for calculation of flight velocity v when the horizontal thrust of the rotors is equal to the drag force of the air:

$$v = \sqrt{2 \cdot tan\theta \cdot mg \big/ \rho c_d S}, \tag{11}$$

where m is the quadcopter's mass, g is the gravitational constant (9.81 m/s^2), ρ is the density of air (1.22 kg/m^3), c_d is the aerodynamic drag coefficient, S is the frontal cross-sectional area of the quadcopter, and θ is the quadcopter's pitch angle. Parameters c_d and S depend on the shape and size of a quadcopter and are difficult to determine analytically.

From equations (7) and (8), the thrust of the quadcopter rotors is proportional to the square of their rotational speeds. The pitch angle θ [15] depends on the difference between the rear and front motor thrusts. It can be assumed that in an ideal case without cross winds, both rear motors rotate at the same speed ω_{rear} and both front motors rotate at the same speed ω_{front}. In this case, the thrust of both rear motors is the same and can be expressed as T_{rear}. The same assumptions can be made and are valid for the front motors, whose thrust is expressed as T_{front}. Taking this into account, the pitch angle θ can be expressed as

$$tan\theta = \frac{T_{rear}}{T_{front}} - 1 = \left(\frac{\omega_{rear}}{\omega_{front}} \right)^2 - 1. \tag{12}$$

Equations (11) and (12) can be used to calculate the necessary rotation speed difference between the rear and front motors. For measurements and analysis, the small quadcopter DJI Spark was used. For this quadcopter, the manufacturer states the maximum velocity and pitch angle of 50 km/h and 35 degrees, respectively. Using these data, equation (11) and the mass of the quadcopter, which equals 300 grams, it is possible to calculate the $c_d S$ product, which is approximately 0.02. For the pitch angle of 35 degrees, from equation (12), the ratio of the rear and front motors' rotation speeds would be 1.3. For example, when the quadcopter hovers at a certain height with all motors rotating at 11,500 revolutions per minute (RPM), when it begins to fly forward from this position with a velocity of 50 km/h, the rear motors will

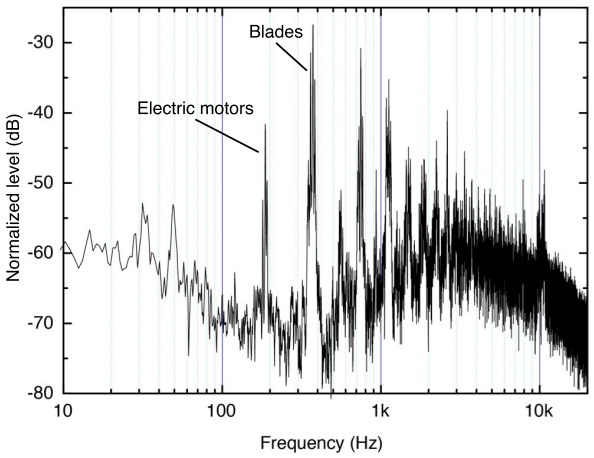

FIGURE 3. Average frequency spectrum of quadcopter's sound when it was hovering (recorded in acoustically treated room, at 1.5 meter height and 1 meter in front of a microphone).

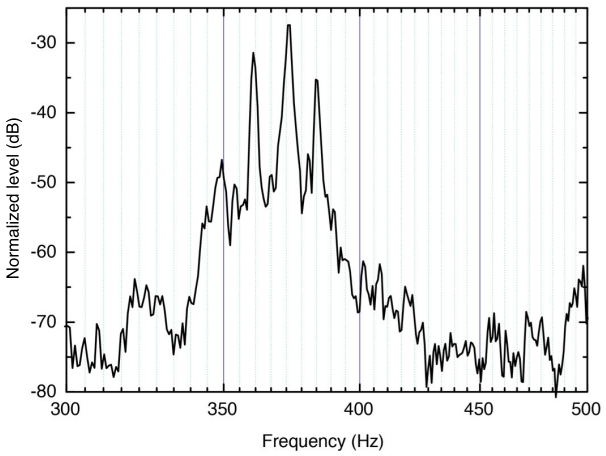

FIGURE 4. Enlarged frequency spectrum from Figure 2 around the most prominent spectrum lines.

rotate at 13,000 RPM, and the front motors will rotate at 10,000 RPM. Similar results can be calculated for other quadcopters of different sizes and maximum speeds. In any case, according to equation (12), for pitch angles ranging from 0 to 45 degrees, this rotation speed ratio can be from 1 to 1.41. With pitch angles higher than 45 degrees, forward thrust would become higher than the thrust necessary to maintain a quadcopter at a certain height, and these pitch angles are avoided.

This paper takes into account and analyzes the frequency spectrum of emitted sound to determine another feature that could be significant for the detection of quadcopter sound signatures. The aim was to measure and determine if these changes in motor rotation speeds could be detected in the frequency spectrum and if they could be connected with the quadcopter motion velocity. The results of this analysis could lead to an efficient method and algorithm for processing recorded quadcopter sounds with the final purpose of detection in different acoustic environments.

III. MEASUREMENTS

As mentioned previously, for the measurements and analysis presented in this paper, a DJI Spark quadcopter was used. This particular quadcopter was selected because it is a good representative of small, popular quadcopters. Furthermore, this quadcopter has a feature that saves various data about flights in time, including changes in revolutions per minute (RPM) for all four electric motors. This feature allowed us to connect RPM with frequency components of the emitted sounds. Measurements were performed in an acoustically treated room and outdoors in the open field.

First, the quadcopter's sound was recorded and analyzed when it was hovering at heights of 1.5 meters and 1 meter in front of a microphone. Figure 3 shows an average frequency spectrum with a time frame of 1 second. There are two main sources of sound in a quadcopter: electrical motors and blades. Both sources feature a broad spectrum that expands to higher frequencies above 10 kHz. The sound of a rotor has features of an impulse sound, and the used quadcopter had two blades per motor. Therefore, the blades' rotation frequency is double of the electrical motors' rotation frequency, i.e., rotation speed. Information about the rotation speed was taken from data gathered by the quadcopter itself. As an additional precaution, the rotation speed of motors was also measured with a laser noncontact tachometer. It was found that data gathered from the quadcopter correspond to data measured with a tachometer.

The first prominent spectrum line in Figure 3 corresponds to the electrical motor's rotation speed. In this case, during hovering, the rotation speed was approximately 10,750 RPM, which corresponds to a frequency of approximately 180 Hz. The second, higher spectrum line corresponds to the blades' rotation speed, which is double the motors' rotation speed due to two blades per motor.

It is evident that although the quadcopter was hovering, there was a difference in speed among motors. This slight difference in speed can also be seen in the frequency spectrum if we zoom in around prominent spectrum lines. The enlarged part is shown in Figure 4. When sufficient fast Fourier transform (FFT) resolution is used, i.e., less than 20 Hz, instead of a single prominent harmonic, there are four harmonics, and each one corresponds to the rotation speed of each individual motor. Taking this phenomenon into account, further analysis was engaged with different flight regimes.

To better connect the rotation speed of the motors, the sound signal of the quadcopter was recorded for a duration of approximately 25 seconds. During this time, the quadcopter was "forced" to ascend, hover, fly forward and backward and descend. Then, the flight session data about the rotational speeds of all four motors were extracted and compared with the recorded sound signal.

Figure 5 shows how the motors' rotation speeds and frequency spectra change over a certain time period during forward-backward flight and hovering. As seen,

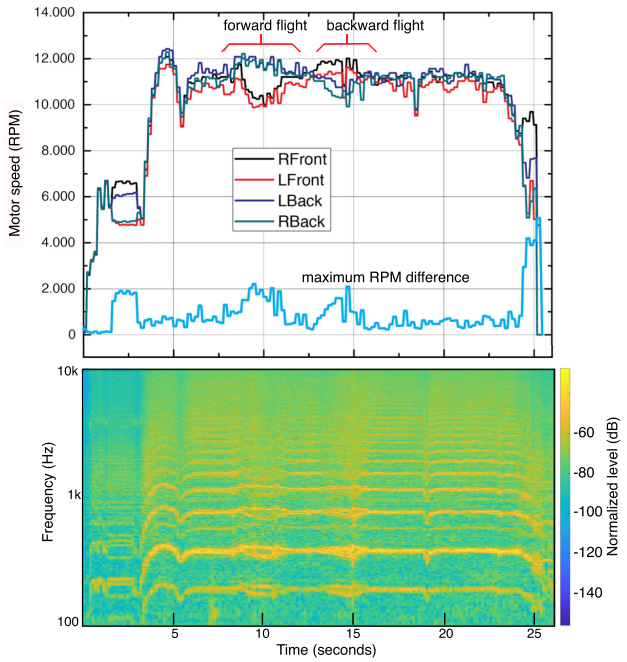

FIGURE 5. (Upper) motor speed versus time; (lower) spectrogram of the quadcopter's sound signal (quadcopter_sound.wav).

the differences in the front and rear motors' rotation speeds increase together with the increase in the quadcopter's forward or backward velocity. When the quadcopter was hovering in place, the frequency spectrum was similar to any impulse sound, as in Figure 3. On the other hand, when the quadcopter was moving, the frequency spectrum changed slightly. In the case of forward flight, the rear motors must rotate faster than the front motors, and the intensity of their spectral lines is higher. This difference in the sound frequency spectrum is characterized by the splitting of prominent spectral lines. This can be connected to the splitting of the front and rear motors' rotation speeds indicated on the rotation speed diagram (shown in the upper part of Figure 5). The analysis showed that the sound signal frequency spectra of a hovering quadcopter and moving quadcopter are significantly different.

A similar conclusion could be drawn from analyzing the changes in the motors' rotation speeds and sound frequency spectra in the case of left-right flight.

From these measurements, it can be concluded that the rotation speed of the quadcopter's motors determines the frequency spectrum of its sound signal. Thus, from the frequency spectrum, a characteristic feature arises. When a quadcopter flies forward, backward, left or right, or in a combination of these regimes, there is an obvious splitting, or a fork line, in the frequency spectrum. To emphasize this trait, the maximum RPM difference between the fastest and slowest rotating electric motors was calculated, which is marked with a blue line in the upper part of Figure 5. In theory, when a quadcopter is not moving, this difference would be zero, i.e., the ratio between the rear and front motors' rotation speed would be 1, as given in equation (12). On the other hand, when quadcopter is moving, this difference could indicate its ground velocity. This is the core objective of this research—finding a method to detect the quadcopter from its sound signal, taking into account spectral line splitting, which would distinguish these UAVs from other surrounding noise sources.

IV. ALGORITHM

From the analysis of the frequency spectrum of the quadcopter's sound, we attempted to extract the sound, which is different from the standard signature extracted from the frequency spectral analysis, which uses the detection of harmonics and their ratios [16]–[20]. The principal idea was to attempt to detect the difference of close frequency components. As seen from the sound frequency spectrum, there are always close frequency components around the harmonics that correspond to the RPM of electric motors and quadcopter blades. Even when a quadcopter hovers, there are small differences in RPM among the four electric motors. When a quadcopter flies forward, backward and to the side, these differences are larger. From Figure 5, which shows how RPM changed during the flight of the used quadcopter, the largest difference appears when the quadcopter was flying forward and is equal to approximately 2,000 RPM, and the maximum ratio of rotation speeds rear and front motors was 1.2. Using this ratio and equation (12), it is possible to calculate the pitch angle. Inserting the calculated pitch angle in equation (11), it is possible to obtain the corresponding velocity. Using the previously calculated $c_d S$ product and physical data for the quadcopter used, the horizontal velocity equals 10.3 m/s, which is 37 km/h. This rotation speed difference corresponds to the basic harmonic of electric motors of 33 Hz and 66 Hz in the case of quadcopter blades. In the case of higher-order harmonics, these frequencies would be 99 Hz, 133 Hz, 266 Hz, and so on.

In the frequency domain, observing Figure 5, these frequency differences could be calculated by finding the maximum frequency components and determining how they change in time. In real conditions, when a quadcopter flies surrounded by other noise sources, the detection of maximum frequency components that correspond to the RPM of electric motors would be a tedious task.

Therefore, this research is focused on sound signal processing in the time domain. According to mathematics, a function that produces a frequency difference is a nonlinear function of even order, such as the following quadratic function:

$$y(t) = x(t)^2. \tag{13}$$

If we assume that the signal consists of two signals with frequencies ω_1 and ω_2 and amplitudes A and B (we omit relative phases for simplicity, without loss of generality)

$$x(t) = A\cos(\omega_1 t) + B\cos(\omega_2 t), \tag{14}$$

then, according to trigonometric functions, the resulting signal will have the following form:

$$y(t) = A^2 + B^2 + \frac{1}{2}A^2 cos(2\omega_1 t) + \frac{1}{2}B^2 cos(2\omega_2 t) + ABcos[(\omega_1 - \omega_2)t] + ABcos[(\omega_1 + \omega_2)t]. \quad (15)$$

The effects of applying a nonlinear transfer function lead to a doubling of basic harmonics, a production of difference frequencies and a direct current (DC) component.

The frequency content of the quadcopter's sound signal is rich with harmonics, and passing this signal though the given quadratic function would result in many additional spectral lines. Taking this into account, and for the sake of argument, the sound signal of a quadcopter can be represented with the following simplified equation while neglecting the phase:

$$x(t) = \sum_{n=1}^{\infty} [A_1 cos(n\omega_{M1}t) + A_2 cos(n\omega_{M2}t) + A_3 cos(n\omega_{M3}t) + A_4 cos(n\omega_{M4}t)], \quad (16)$$

where ω_{M1} to ω_{M3} are rotation frequencies of the motors with signal amplitudes A_1 to A_4 with indexes according to Figure 2. In a case when a quadcopter flies forward, the rotation speed of both rear and front motors should be the same ($\omega_1 = \omega_2 = \omega_{front}$ and $\omega_3 = \omega_4 = \omega_{rear}$), and equation (14) can be written as

$$x(t) = \sum_{n=1}^{\infty} [cos(n\omega_{front}t) + cos(n\omega_{rear}t)]. \quad (17)$$

This still includes a large number of harmonics, which could be reduced using a bandpass filter on a recorded signal, and equation (17) would be similar to equation (14). For example, taking into account that the rotation speed of small and medium quadcopters ranges from 4,000 to 12,000 RPM, only frequencies in the range from 100 Hz to 500 Hz can be included. This is the range of frequencies corresponding to the rotation speed of the blades, whose sound level is dominant (see Figure 5).

Figure 6 shows a flowchart of the proposed algorithm using a real-time signal. First, the recorded signal is bandpass filtered between 100 Hz and 500 Hz, which will include the two largest sound signals of a quadcopter: the motor and blade. Then, the signal is passed through a nonlinear function, which will result in new spectral components, including the frequency differences. Then, the processed signal is analyzed in the frequency domain by comparing new low-frequency and high-frequency components. If the high-frequency difference corresponds to the low-frequency component, the recorded signal could be connected with a quadcopter.

Figure 7 shows a spectrogram of the bandpass filtered sound signal of the quadcopter used in three flight regimes: hovering and forward-backward flight. Bottom spectral lines correspond to the first harmonic of electric motors and upper lines to the blades. In addition, Figure 7 shows the splitting of spectral lines in the case of forward and backward flight. From Figure 7, in the case of forward flight, the maximum frequency splitting is approximately $\Delta f_1 = 80$ Hz. For the backward flight, this difference is somewhat lower, and it is

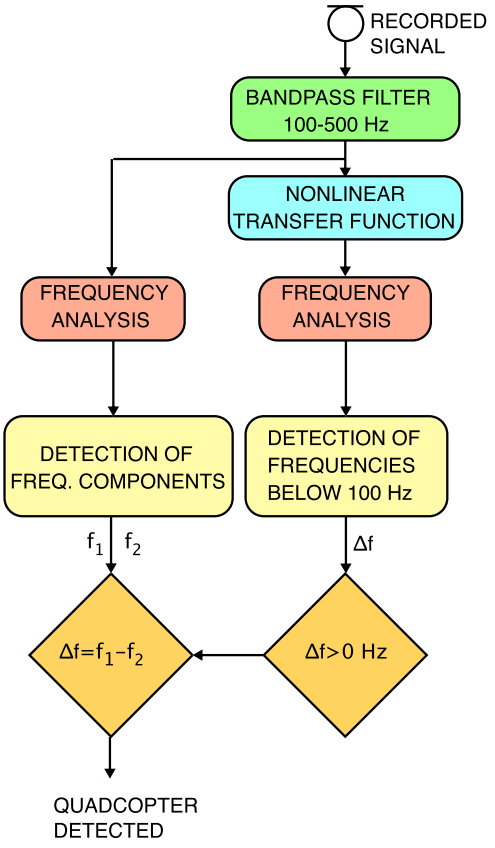

FIGURE 6. Flowchart of the proposed algorithm.

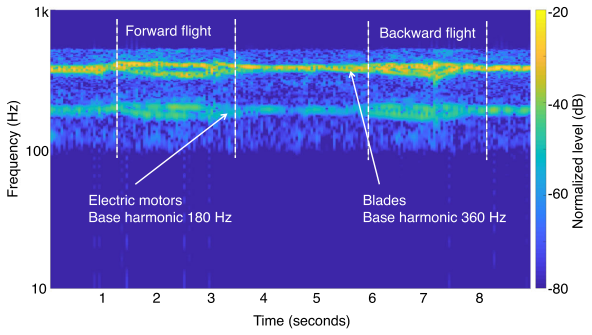

FIGURE 7. Spectrogram of filtered quadcopter sound signal where the upper spectral lines correspond to blades and the lower spectral lines correspond to electric motors.

approximately $\Delta f_2 = 70$ Hz, which in general depends on quadcopter's ground velocity.

The basic frequency lines when the quadcopter hovers are $f_1 = 180$ Hz and $f_2 = 360$ Hz. In the case of forward flight, there are four spectral lines, $f_1 \pm \Delta f_1/2$ and $f_2 \pm \Delta f_2/2$.

The processing of the filtered signal with a nonlinear function, such as in equation (13), would result in a signal with several new spectral components. In theory, new spectral components, in the case when quadcopter hovers are f_2-$f_1 = 180$ Hz, $f_2 + f_1 = 540$ Hz, $2f_1 = 360$ Hz, $2f_2 = 720$ Hz and a DC component. In the case when the quadcopter flies forward, at the point where the frequency splitting difference is the largest, there are several new frequency components,

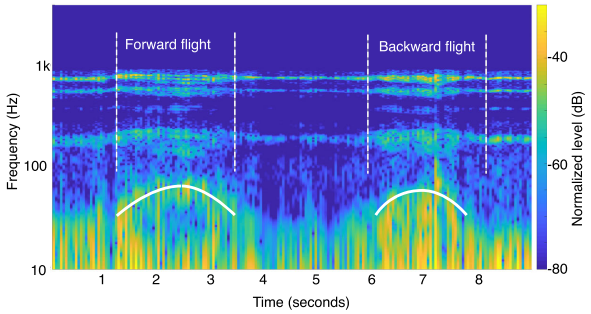

FIGURE 8. Spectrogram of the quadcopter signal after processing using equation (11), where white lines mark frequency difference signals.

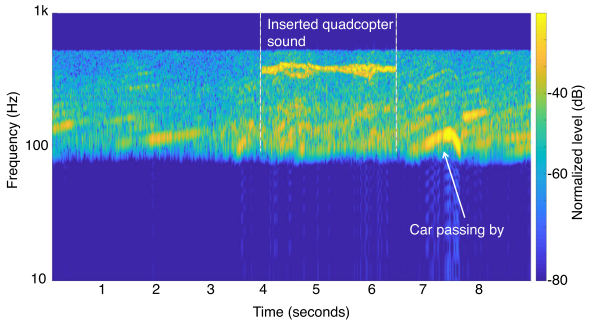

FIGURE 9. Spectrogram of the quadcopter's sound signal mixed with traffic noise signal.

and among them is the difference of the base frequency splitting, which is 80 Hz.

Figure 8 shows the resulting spectrogram. The white lines show the frequency difference spectral lines in the case of forward and backward flight, which correspond to the frequency difference in Figure 7. The processed signal also includes a DC component, as shown in equation (15). This DC component could represent a problem if insufficient frequency resolution is used for analysis at these low frequencies. The frequency resolution used in Figure 8 was 0.33 Hz. This is a very low frequency resolution, and in the case of real-time processing systems, it represents quite a load. This load can be reduced by retaining the same frequency resolution by reducing the sampling rate of the recorded signal with a lower number of FFT points.

This splitting of the frequencies for forward and backward and left and right flight is a characteristic feature of quadcopters, that is, flying vehicles with four or more motors with blades, and could be used for the reliable detection of quadcopters. The quadcopter's signal used for this processing is recorded in a noise-free environment, i.e., an acoustically treated room. In real-life situations, this noise-free environment is extremely challenging to ensure, since a quadcopter's sound will be mixed with noise. Therefore, it is necessary to analyze this signal when it is surrounded by noise.

V. ANALYSIS OF THE SOUND SIGNAL AND NOISE

To analyze the proposed algorithm, the recorded sound of the quadcopter was mixed with traffic noise and evaluated to see if the quadcopter's sound signature could be detected in the spectrogram. Traffic noise was chosen because it is the most common type of noise with which the quadcopter's sound signal would be surrounded in real-case scenarios. The traffic noise is characterized by mainly low-frequency content and spreads to approximately 1 kHz, which is slightly above the main frequency components of the quadcopter's sound. Three levels of the quadcopter's sound signal were selected, which had an average level difference between the quadcopter's sound signal and noise sound signal of 3 dB, 0 dB and −3 dB.

Figure 9 shows a spectrogram of the quadcopter's sound signal mixed with the traffic noise signal, with the same average level. The quadcopter's sound is inserted in the time interval between the 14th and 23rd seconds, as indicated in Figure 9. The combined signal in Figure 9 is bandpass filtered from 100 to 500 Hz to reduce the number of spectral components of the quadcopter's sound signal. This filtering has allowed us to focus on only two prominent spectral lines of the quadcopter's sound signal. On the other hand, this filtering removed any low-frequency noise components that could be seen in the processed signal. The traffic noise signal, among others, includes a relatively intense sound of a passing car, with prominent first and subsequent harmonics. The quadcopter's sound signal is intentionally placed before the car's sound signal, which permitted the comparison of signal levels of both signals to see if the quadcopter's signal could be differentiated from the car's signal.

The mixed signal, with all three levels of the quadcopter's sound signal, was processed with a simple quadratic function shown in equation (13). Figure 10 shows spectrograms of the processed mixed signals with three levels of the quadcopter's signal.

As expected, as the quadcopter signal becomes lower, it is harder to detect the resulting low-frequency components, corresponding to frequency splitting when the quadcopter flies forward or backward. When the surrounding noise does not include impulse signals, such as in the case of a passing car, with several spectral components, the quadcopter's signal is visible up to 3 dB below the average noise level. Below that level, it is difficult to distinguish the quadcopter's signal from the car's sound signal, which also exhibits low-frequency components after processing. Higher spectral components of the quadcopter's sound are visible up to the lowest level of the mixed signal. It can be concluded that the proposed algorithm, for low signal-to-noise ratios, should include analysis of both low- and high-frequency content. The final algorithm should simultaneously analyze if there are prominent low-frequency and higher frequency components. The low-frequency components should correspond to the higher frequency component differences, and then, it could be concluded that this is the quadcopter's sound signature.

This detection of the sound signature could be combined with other detection methods. For example, in combination with a radar signal, which would detect an object at a certain distance, the analysis of sound from this direction based on

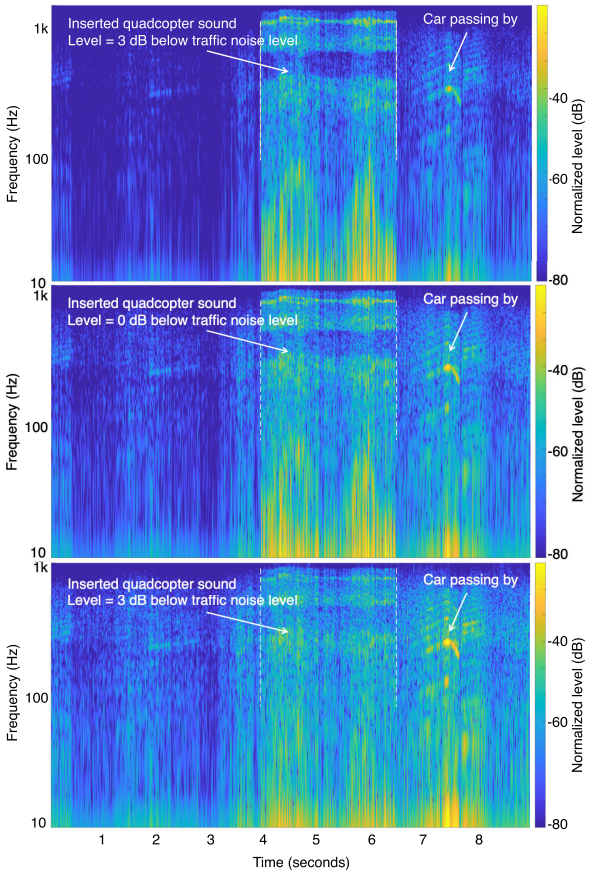

FIGURE 10. Spectrogram of the mixed signal after processing with a nonlinear function for three levels of the quadcopter's sound.

this specific sound feature could improve the precision and detection reliability. The signal-to-noise ratio is the same as in cases of other methods for quadcopter sound analysis; however, processing with a nonlinear function enables the average level of the quadcopter sound to be even lower than the surrounding noise level.

VI. CONCLUSION

A quadcopter's sound signal was recorded when the quadcopter was flying in different regimes (forward-backward, left-right). The recorded sound signals were analyzed in the frequency domain, and it was found that the frequency spectrum corresponds to the rotation speed of the four quadcopter motors. When quadcopters hover at a certain height, the motors' rotation speeds are mainly constant, and the frequency spectrum of the quadcopter's sound signal is similar to any harmonic sound source with a rich frequency spectrum. The frequency spectrum of its sound signal is different when the quadcopter is moving. In this case, there is visible spectrogram line splitting, which corresponds to the difference in rotation speed among motors. When a quadcopter flies forward, the rear motors rotate faster than the front motors, and vice versa. Even when a quadcopter hovers, there is a slight difference in the rotation speeds because the quadcopter must constantly adjust the rotation speeds to stay in a certain flight regime.

This aforementioned fact is used to propose an algorithm for the detection of a quadcopter when it is surrounded by noise, detecting its characteristic sound signature. The algorithm includes passing the recorded audio signal through a nonlinear function, which will identify the differences in the signal's spectral components. Analysis showed that with the corresponding frequency resolution and signal-to-noise ratio, it is possible to distinguish the quadcopter signal from the surrounding noise.

Further analysis and research will focus on a possible extension and potential improvement of the algorithm described in this paper. An extension of the proposed algorithm will rely on different noise reduction methods for the recorded quadcopter's signal in the case of a low signal-to-noise ratio to facilitate the detection of its sound signal. A potential improvement could also be obtained by implementing another nonlinear function, which will provide new or additional low-frequency components with higher levels and enable the definition of the advanced algorithm for recognition of the quadcopter's sound print.

REFERENCES

[1] M. Ritchie, F. Fioranelli, and H. Borrion, "Micro UAV crime prevention: Can we help Princess Leia?" *Crime Prevention in the 21st Century: Insightful Approaches for Crime Prevention Initiatives*, B. LeClerc and E. U. Savona, Eds. New York, NY, USA: Springer, pp. 359–376, doi: 10.1007/978-3-319-27793-6_21.

[2] *Gatwick Airport Drone Incident*. Accessed: Dec. 1, 2019. [Online]. Available: https://en.wikipedia.org/wiki/Gatwick_Airport_drone_incident

[3] M. Kratky and L. Fuxa, "Mini UAVs detection by radar," in *Proc. Int. Conf. Military Technol. (ICMT)*, Brno, Czech Republic, May 2015, pp. 1–5.

[4] F. Hoffmann, M. Ritchie, F. Fioranelli, A. Charlish, and H. Griffiths, "Micro-Doppler based detection and tracking of UAVs with multistatic radar," in *Proc. IEEE Radar Conf. (RadarConf)*, Philadelphia, PA, USA, May 2016, pp. 1–6.

[5] F. H. Schmitz, "Aeroacoustics of flight vehicles: Theory and practice, rotor noise," Ames Research Center, NASA, Washington, DC, USA, WRDC Tech. Rep. 90-3052 and N92-10600, Aug. 1991, Vol. 1.

[6] L. Shi, I. Ahmad, Y. He, and K. Chang, "Hidden Markov model based drone sound recognition using MFCC technique in practical noisy environments," *J. Commun. Netw.*, vol. 20, no. 5, pp. 509–518, Oct. 2018.

[7] J. Mezei, V. Fiaska, and A. Molnar, "Drone sound detection," in *Proc. 16th IEEE Int. Symp. Comput. Intell. Informat. (CINTI)*, Budapest, Hungary, Nov. 2015, pp. 333–338.

[8] A. Bernardini, F. Mangiatordi, E. Pallotti, and L. Capodiferro, "Drone detection by acoustic signature identification," in *Proc. Int. Symp. Electron. Imag.*, San Francisco, CA, USA, 2017, pp. 60–64.

[9] S. Jeon, J. W. Shin, Y. J. Lee, W. H. Kim, Y. H. Kwon, and H. Y. Yang, "Empirical study of drone sound detection in real-life environment with deep neural networks," Jan. 2017, *arXiv:1701.05779*. [Online]. Available: https://arxiv.org/abs/1701.05779

[10] H. L. Chan and K. T. Woo, "Design and control of small quadcopter system with motor closed loop speed control," *Int. J. Mech. Eng. Robot. Res.*, vol. 4, no. 4, pp. 287–292, Oct. 2015.

[11] R. Mahony, V. Kumar, and P. Corke, "Multirotor aerial vehicles: Modeling, estimation, and control of quadrotor," *IEEE Robot. Automat. Mag.*, vol. 19, no. 3, pp. 20–32, Sep. 2012.

[12] G. M. Hoffman, H. H. Huang, S. L. Waslander, and C. J. Tomlin, "Quadrotor helicopter flight dynamics and control: Theory and experiment," in *Proc. AIAA Guid., Navigat. Control Conf. Exhibit*, Hilton Head, SC, USA, Aug. 2007, pp. 20–23.

[13] N. Intaratep, W. N. Alexander, and W. J. Davenport, "Experiment study of quadcopter acoustics and performance at static thrust conditions," in *Proc. 22nd AIAA/CEAS Aeroacoustics Conf.*, Lyon, France, 2016, p. 2873.

[14] S. Yadav, M. Sharma, and A. Borad, "Thrust efficiency of drones (quad copter) with different propellers and their payload capacity," *Int. J. Aerosp. Mech. Eng.*, vol. 4, no. 2, pp. 18–23, Apr. 2017.
[15] J. S. Reid, "Drone flight—What does basic physics say? In physics lectures," Univ. Aberdeen, JSR, Bengaluru, Karnataka, Tech. Rep. Version 2b, Jul. 2018. [Online]. Available: https://homepages.abdn.ac.uk/nph120/meteo/DroneFlight.pdf
[16] G. Sinibaldi and L. Marino, "Experimental analysis of the noise of propellers for small UAV," *Appl. Acoust.*, vol. 74, pp. 79–88, Jan. 2013.
[17] V. Kartashov, V. Oleynikov, I. Koryttsev, O. Zubkov, S. Babkin, and S. Sheiko, "Processing and recognition of small unmanned vehicles sound signals," in *Proc. PIC*, Kharkiv, Ukraine, Oct. 2018, pp. 392–396.
[18] N. Kloet, S. Watkins, and R. Clothier, "Acoustic signature measurement of small multi-rotor unmanned aircraft system," *Int. J. Micro Air Vehicles*, vol. 9, no. 1, pp. 3–14, 2017.
[19] J. Kim, C. Park, J. Ahn, Y. Ko, J. Park, and J. C. Gallagher, "Real-time UAV sound detection and analysis system," in *Proc. IEEE Sensors Appl. Symp. (SAS)*, Glassboro, NJ, USA, Mar. 2017, pp. 13–15.
[20] A. Sedunov, D. Haddad, H, Sallooum, A. Sutin, N. Sedunov, N. Sedunov, and A. Yakubovskiy, "Stevens drone detection acoustic system and experiments in acoustics UAV tracking," in *Proc. IEEE Int. Symp. Technol. Homeland Secur. (HST)*, Woburn, MA, USA, Nov. 2019, pp. 5–6.

IVAN DJUREK (Member, IEEE) was born in Zagreb, Croatia, in 1972. He received the B.Sc. and M.Sc. degrees in electrical engineering from the University of Zagreb, Croatia, in 1996 and 2000, respectively, and the Ph.D. degree in electrical engineering from the University of Zagreb, in 2003. He is currently a Professor with the Department of Electroacoustics, Faculty of Electrical Engineering and Computing, University of Zagreb. His main research interests include audio equipment, transducers, and audio signal processing.

ANTONIO PETOSIC was born in Požega, in 1979. He received the B.Sc. and Ph.D. degrees from the Faculty of Engineering and Computing, University of Zagreb, in 2002 and 2008, respectively. He is currently working as an Associate Professor with the Department of Electroacoustics, Faculty of Electrical Engineering and Computing, University of Zagreb. His main areas of his interests are the characterization of electroacoustic transmitters and systems.

SANJA GRUBESA was born in Rijeka, Croatia, in 1980. She received the B.Sc. and Ph.D. degrees from the Faculty of Engineering and Computing, University of Zagreb, in 2004 and 2011, respectively. She is currently a Research Assistant with the Department of Electroacoustics, Faculty of Electrical Engineering and Computing, University of Zagreb. Her main research interests are noise, noise barrier, and optimization.

MIA SUHANEK was born in Zagreb, Croatia, in 1983. She received the B.Sc. and Ph.D. degrees from the Faculty of Engineering and Computing, University of Zagreb, in 2006 and 2013, respectively. She is currently a Research Assistant with the Department of Electroacoustics, Faculty of Electrical Engineering and Computing, University of Zagreb. Her main research interests are acoustic environments, soundscape, and psychoacoustic modeling.